

OCEANPAL[®], A GPS-REFLECTION COASTAL INSTRUMENT TO MONITOR TIDE AND SEA-STATE

S. Dunne, F. Soulat, M. Caparrini, O. Germain, E. Farrès, X. Barroso⁺ and G. Ruffini

*Starlab Barcelona S.L.
Muntanya del Tibidabo, Camí de l'Observatori s/n
08034 Barcelona, Spain
Email: olivier.germain@starlab.es*

*⁺Universitat Autònoma de Barcelona
Hospital de la Vall d'Hebron, Psg/ Vall d'Hebron 119, 129
08035 Barcelona, Spain*

INTRODUCTION

The Global Navigation Satellite Systems (GNSS, such as the GPS and GLONASS constellations) and their augmentation systems (WAAS, EGNOS) constitute premium sources of opportunity for passive remote sensing. By 2010, after the deployment of the European Galileo constellation, more than 50 GNSS satellites will be emitting self-calibrating, dual-frequency, rain-immune, L-band spread spectrum signals with long-term availability and stability.

The use of GNSS reflections (GNSS-R) for sea-surface monitoring is a bistatic radar technique only requiring a receiving system. The concept was initially proposed by M. Martin-Neira in 1993 [1] and has, since then, been successfully implemented in coastal receivers [2,3], in aircraft [4-7] and recently, in space [8]. The potential applications include sea-surface altimetry, sea-state, surface roughness, surface currents and salinity, both for scientific and operational oceanography.

In this paper, we present Oceanpal[®], a GNSS-R sensor developed by Starlab for operational coastal monitoring. It is an inexpensive, all-weather, dry and passive concept which can be deployed on multiple platforms, static (coasts, harbors, off-shore), and slowly moving (boats, floating platforms, buoys). In its present form, Oceanpal[®] can deliver two kinds of Level-2 products: the sea-surface height and the significant wave height.

THE INSTRUMENT

Oceanpal[®] features a pair of low gain L-band antennas. The RHCP zenith antenna collects the direct GPS signal while the LHCP nadir antenna registers its sea-surface reflections. A raw data burst of some minutes is acquired in each channel, down-converted and one-bit sampled. These direct and reflected raw data are first fed to the Starlight[®] module, an virtual pair of (software) GPS receivers which detect and track the GPS signals in the direct (master) channel and despreads the reflected signals in the slave channel. The result of this processing is a set of direct/reflected electromagnetic field time series for each satellite in view, plus the GPS time reference (Level-0 data).

The Level-0 data are then further processed to yield two kinds of Level-2 products: the sea-surface height and the significant wave height. These products are stored in a database of the data management unit which also acts as a web server. They can be accessed remotely via a regular web browser interface.

COASTAL ALTIMETRY

Altimetry with GNSS-R consists in measuring the delay between the times of arrival of a direct GNSS signal and its reflection over the sea surface. To this end, both code and carrier phase delays can be estimated. Code altimetry is less

precise than phase altimetry but more robust to sea-state conditions. Phase altimetry is presented here as a mean to perform altimetry over calm water surfaces, like over lakes or inside a harbour.

In order to eliminate the modulations of the GPS navigation message and all errors (propagation, clocks, residual Doppler, etc.) common to both signals, we form the *interferometric* field $I(t)$ as the ratio of the reflected $I(t)$ and the direct $R(t)$ signals.

For each satellite in view (indexed by p), the phase of the interferometric field is proportional to the reflected signal extra path distance. By simple geometrical considerations, this phase can be linked to $h(t)$, the height of the receiver over the reflective surface signal and $\varepsilon_p(t)$, the elevation angle of the satellite:

$$\Phi_p(t) = 2k h(t) \sin \varepsilon_p(t) \quad (1)$$

where k is the wave number of the GPS carrier frequency. In reality, the hardware will also introduce an additional phase term, leaving:

$$\Phi_p(t) = 2k h(t) \sin \varepsilon_p(t) + \theta(t) \quad (2)$$

In (3) the phase offset θ is implicitly common to all satellites but explicitly time-dependent, which accounts for drift. For reasonably good hardware this drift should be small enough to consider the phase offset constant over short time-spans. The difficulty in solving for h and θ , although the later does not have to be solved explicitly, is due to the ambiguities resulting from the modulo- 2π wrapping of the phase.

For a set of measurements, the relevant interferometric information is a set of unitary complex values: $e^{i\tilde{\phi}_p(t)}$. In order to jointly estimate h and θ , we build the error function:

$$C(h, \theta) = \sum_{p,t} \left| e^{i\tilde{\phi}_p(t)} - e^{i\phi_p(t)} \right| \quad (3)$$

where $\Phi_p(t)$ is the phase model of eq.(3) which implicitly depends on h and θ and the elevation angle time series. The figure below shows a simulated cost function (i.e. the phase measurements are generated according to the model of eq. (3)) in a case with 6 satellites of elevations: 15, 24, 36, 44, 68 and 78 degrees. The difficulty discussed above manifests here through the presence of several local minima: in a noisy situation. These spurious minima could strongly affect the estimation accuracy. However, we see that with a large span of elevation values, the function exhibits a deep global minimum which guarantees precise estimation. Note in addition that the cost function is barely sensitive to the phase offset, a good point.

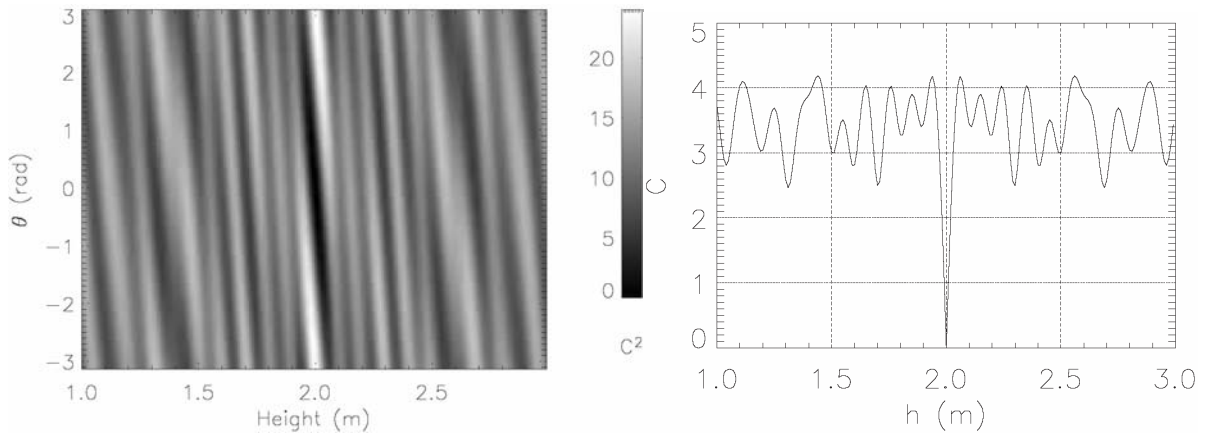


Fig. 1. Example of simulated cost function obtained with six satellites in view. The height is 2.00 m and the phase offset is null. Left: full 2D map. Right: cut at $\theta=0$.

The Villagarcía Campaign

This tide estimation scheme was applied during an experimental campaign in the Port of Villagarcía (Galicia, Spain). The campaign was carried out in July 2004 in collaboration with Puertos del Estado, at the Villagarcía Port. The site was chosen because of the presence of a reliable ground truth (tide gauge), for its position in the innermost part of the harbour and finally, for the magnitude of tide events in that region.

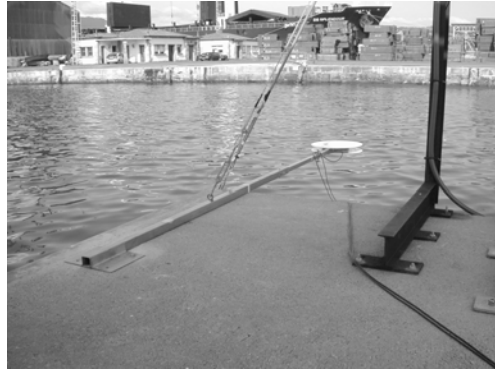


Fig. 2. The antenna (white dishes) mounted on the pier at Villagarcía.

The height over sea surface was estimated every 30 minutes, on the basis of 2 minutes of collected data. The coherent integration time used to disperse the GPS signals was 20 milliseconds. An astronomical tidal model was used as first guess for the algorithm initialisation. The quality check of the result was performed using as ground truth the tidal data provided by a RADAR tide gauge, averaged over intervals of 2 minutes.

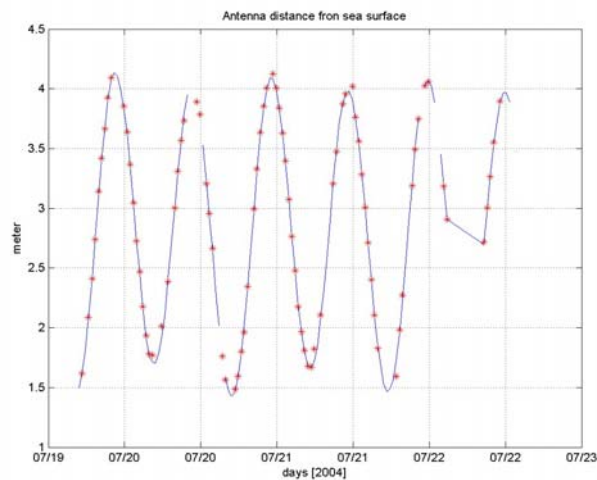


Fig. 3. Ground truth (solid line) and Oceanpal estimated values (dots).

The sea surface height estimation is shown in Fig. 3. The standard deviation obtained with respect to the ground truth is of 3.1 cm. On average, 25% of data had to be rejected, due to the complex geometry of the harbour environment, affected by multipath.

COASTAL SEA STATE

The retrieval of sea-state with coastal GNSS-R relies on the measurement of the interferometric field coherence time which is expected to be a decreasing function of ocean agitation. This coherence time is defined as the width of the autocorrelation function, given by

$$\Gamma(\Delta t) = \frac{1}{2T} \int_{-T}^T I^*(t) I(t + \Delta t) dt, \quad (4)$$

where T is the duration of the data take. Assuming a Gaussian probability distribution for the surface elevations and focusing on short time shifts Δt , the autocorrelation function can be approximately written (see [3] for details) as

$$\Gamma(\Delta t) \approx A(\sigma_z, l_z, \varepsilon, G_r) \cdot e^{-4k^2 \sigma_z^2 \frac{\Delta t^2}{2\tau_z^2} \sin^2 \varepsilon}, \quad (5)$$

where σ_z is the sea surface elevation standard deviation, l_z is the sea surface autocorrelation length, ε is the elevation of the satellite, G_r is the gain pattern of the receiving antenna, τ_z is the correlation time of the surface. The coherence time τ_I of the interferometric field is then identified to be

$$\tau_I = \frac{\tau_z}{2k\sigma_z \sin \varepsilon} = \frac{\lambda}{\pi \sin \varepsilon} \frac{\tau_z}{SWH}, \quad (6)$$

where the significant wave height (SWH) has been introduced.

Equation (6) states that the coherence time of the interferometric field is proportional the ratio between τ_z and SWH , i.e. the inverse of an effective ‘‘surface velocity’’. The surface coherence time τ_z and standard deviation SWH are not independent parameters, but linked by a non-trivial relationship depending on sea state, sea maturity, fetch, bathymetry, etc. In coastal zones, this function will be harder to estimate from theory and a semi-empirical approach is preferred. Our Level-2 algorithm, based on calibrated measurements, writes

$$SWH = SWH_0 + \frac{\alpha}{k\tau_I \sin \varepsilon - \beta}, \quad (7)$$

where SWH_0 , α and β are the calibration parameters.

The Barcelona Port Test Bed

An Oceanpal[®] prototype is presently deployed at the Meteorological station of Porta Coeli in the port of Barcelona and has been taking continuous measurements since December the 30th of 2004. The station is located on the outermost port breaker and the antennas are mounted 25 m above the open sea surface. In this site, the satellite visibility is limited by the presence of the pier, which can add some ground multipath reflections in certain receiving geometries. Consequently, we had to restrict the measurements to a masking angle of [10 to 35 degrees] in elevation and [55 to 165 degrees] in azimuth. This leads to an observation area of about 100 meter radius onto the open sea. A TRIAXYS buoy located near the delta of the Llobregat river (some 10 miles south from the experimental site) delivered hourly SWH and Mean Wave Period values. These data were used during the calibration campaign to infer the relationship between τ_z and SWH and hence, design the semi-empirical algorithm of eq. (7). In the present configuration, one-minute data bursts are taken every 15 minutes to estimate SWH . The data can be browsed remotely using the web interface of fig. 5. Fig. 4 shows the correlation plot between the buoy and the Oceanpal estimations obtained after 71 days of measurements. The residual error standard deviation is of the order of 18 cm.

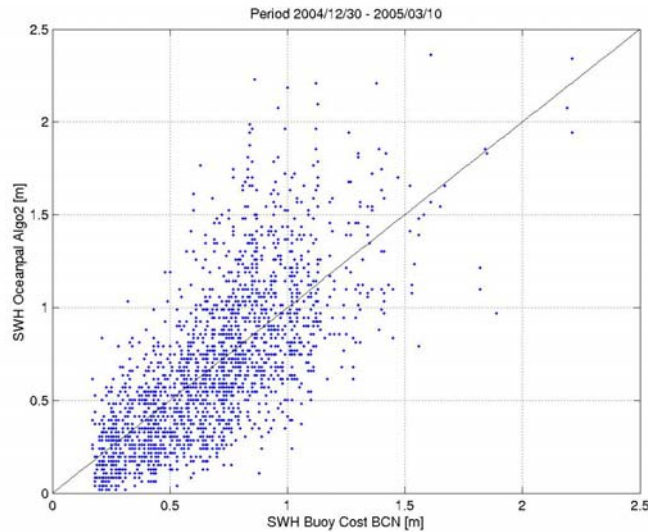


Fig. 4. Oceanpal vs. Buoy SWH measurements.

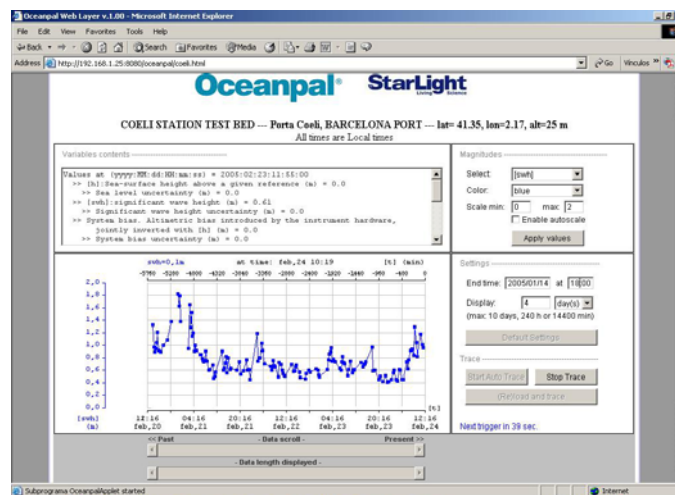


Fig. 5. Oceanpal web interface, allowing remote access to data.

CONCLUSION

In this paper we have presented Oceanpal[®], a GNSS-R instrument for coastal sea-surface monitoring. We have discussed two initial applications: the provision of tide measurements inside a harbour and the estimation of sea-state in open sea from a harbour pier. Both of these measurements are based on the same GNSS-R product: the complex interferometric field, defined as the ratio of the reflected and direct GNSS signals. Two dedicated campaigns have demonstrated precisions of 3 cm and 18 cm for the tide and the *SWH* measurements respectively.

Although not addressed in this paper, several experiments have shown that GNSS-R can also provide information from airborne and spaceborne platforms using code ranging. The combination of ground, air and space receivers exploiting reflected GNSS signals will certainly provide a very solid framework for operational and scientific oceanographic applications in the near future.

ACKNOWLEDGEMENTS

The authors are grateful to Puertos del Estado and the Barcelona Port Authority Environmental Monitoring Department for their support in the experimental campaigns. The deployment at the Barcelona harbour was partially funded by Ifremer under contract BHOPE-4.

All Starlab authors have contributed significantly; the Starlab authors list has been ordered randomly.

REFERENCES

- [1] M. Martín-Neira, “A PASSive Reflectometry and Interferometry System (PARIS): application to ocean altimetry”, *ESA Journal*, 17:331–355, 1993.
- [2] M. Martin-Neira, M. Caparrini, J. Font-Rossello, S. Lannelongue, and C. Serra. “The PARIS concept: An experimental demonstration of sea surface altimetry using GPS reflected signals”, *IEEE Transactions on Geoscience and Remote Sensing*, 39:142-150, 2001.
- [3] F. Soulat, M. Caparrini, O. Germain, P. Lopez-Dekker, M. Taani, G. Ruffini, “Sea State Monitoring using coastal GNSS-R”, *Geophys. Res. Lett.*, Vol. 31, 2004.
- [4] J. Garison, “Wind speed measurements using forward scattered GPS signals”, *IEEE Transactions on Geoscience and Remote Sensing*, 40:0-65, 2002.
- [5] Lowe, S., C. Zuffada, Y. Chao, P. Kroger, J.L LaBreque, and L.E. Young, “5-cm precision aircraft ocean altimetry using GPS reflections”, *Geophys. Res. Lett.*, (29):4359–4362, 2002.
- [6] G. Ruffini, F. Soulat, M. Caparrini, O. Germain and M. Martin-Neira, “The Eddy Experiment: accurate GNSS-R ocean altimetry from low altitude aircraft”, *Geophys. Res. Lett.*, Vol. 31, 2004.
- [7] O. Germain, G. Ruffini, F. Soulat, M. Caparrini, B. Chapron and P. Silvestrin, “The Eddy Experiment II: GNSS-R specularometry for directional sea-roughness retrieval from low altitude aircraft”, *Geophys. Res. Lett.*, Vol. 31, 2004
- [8] S. Gleason, S. Hodgart, Y. Sun, C. Gommenginger, S. Mackin, M. Adjrard, M. Unwin, “Detection and Processing of Bi-Statically Reflected GPS Signals From Low Earth Orbit for the Purpose of Ocean Remote Sensing”, to appear in *IEEE Transactions on Geoscience and Remote Sensing*